Causality violations in cascade models of nuclear collisions

G. Kortemeyer, W. Bauer, K. Haglin, J. Murray, and S. Pratt

NSCL/Cyclotron Laboratory, Michigan State University, East Lansing, Michigan 48824

(Received 1 May 1995)

Transport models have successfully described many aspects of intermediate energy heavy-ion collision dynamics. As the energies increase in these models to the ultrarelativistic regime, Lorentz covariance and causality are not strictly respected. The standard argument is that such effects are not important to final results; but they have not been seriously considered at high energies. We point out how and why these happen, how serious of a problem they may be and suggest ways of reducing or eliminating the undesirable effects.

PACS number(s): 25.75.+r, 24.85.+p

I. INTRODUCTION

Experiments like the upcoming nucleus-nucleus collisions at Brookhaven's Relativistic Heavy Ion Collider will without doubt open new possibilities to study the properties of nuclear matter at extreme pressures and temperatures. Of special interest is the expected phase transition between hadronic and quark-gluon matter. The interpretation of these complex collisions and the possible generation of a quark-gluon plasma poses a major problem: what are the experimental signatures? In an effort to aid the answering of this question a theoretical model for the collision processes that goes beyond a phenomenological description must be developed. One possible microscopic approach is to extend the semiclassical transport theory to high-energy physics [1–8].

Simulations of ultrarelativistic heavy ion collisions inevitably involve both soft and hard processes. Below some energy scale, soft or nonperturbative phenomena necessitate phenomenological description. Uncertainty is duly noted but for the foreseeable future a rigorous theory for soft physics is beyond understanding. However, throughout much of the collision hard processes dominate which are described by elementary interactions between quarks, antiquarks and gluons (partons) as essentially semiclassical particles. After parton initialization according to some reasonably chosen nucleon structure functions, spacetime propagation is accomplished by discretizing time into units Δt_{step} and updating phase space densities according to relativistic transport equations including a crucial collision term.

Scattering processes in this theoretical framework are assumed to be nonretarded which, on a microscopic level, leads to information transport with velocities that can approach $\sqrt{\sigma/\pi}/\Delta t_{step}$, where σ is the parton-parton cross section. That is, it can increase without reasonable bound. As energies for the individual interactions decrease the corresponding cross sections increase. The timestep Δt_{step} is for reasons of convergence chosen to be less than the parton mean free paths divided by their velocities: of the order a few thousandths of a fm/c. Two problems occur immediately: On a macroscopic level a series of subsequent causality violating interactions can lead to shock waves propagating faster than the speed of light. This is clearly unphysical. On a microscopic level the time ordering of the incoming and outgoing partons of a scattering process becomes frame dependent and Lorentz covariance is lost — this also is un-

physical. These two problems are especially serious in ultrarelativistic parton cascades since collision rates are high, and the mean free paths approach the interparticle distance. Problems arise from describing quantum-dynamical processes in a semiclassical picture, and from the demand of Lorentz invariance in an equal-time-character simulation. Where is an acceptable compromise? And what does acceptable mean?

These are the rather technical questions we address in this study, while in [9] we are more focussing on the physics of parton cascade codes. Our paper is organized in the following way. In Sec. II we describe in some detail the origin of superluminous information transport on a macroscopic scale and suggest some first steps to eliminate it. Then in Sec. III we move toward microscopic physics and provide mathematical details for origins of unphysical effects. Whenever cross sections are finite and action-at-a-distance influences particle trajectories these problems inevitably arise. Section IV deals with the resulting frame-of-reference dependence of the simulation. In Sec. V we describe our version of a parton cascade implementation. At this stage we have only initialization and temporal development through much of the hard physics. Later stages including hadronization are ignored since they are outside the scope of this work. Then in Sec. VI we compare several different schemes which reduce or eliminate superluminous transport. Methods include simply blocking collisions or truncations, scaling the cross sections downward while increasing the number of particles, and suppressing low-energy collisions. We also consider so-called wee partons as a different way to define the initial conditions of the simulation, and point out how much this scheme affects causality violating mechanisms. Finally, in Sec. VII we conclude by briefly summarizing, and by discussing the outlook for future studies.

II. MACROSCOPIC CAUSALITY VIOLATIONS

Superluminous macroscopic information transport occurs mainly in the transverse (perpendicular to the beam) direction. The signal can travel over the diameter of the cross section σ in a single time step and then continue this propagation from time step to time step. Transverse signal velocities can therefore reach $\sqrt{\sigma/\pi}/\Delta t_{step}$ over several time steps, one is reminded of a chain of falling dominoes. The situation is depicted in Fig. 1 for such a transport.
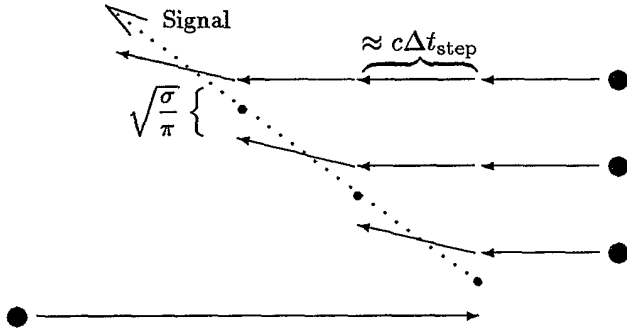
FIG. 1. One particle coming from the left scatters with another particle coming from the right. As part of the model the scattered particles cannot scatter again in this time step. However, one time step later that scattered particle from the right scatters with another particle coming from the right. As a result information from the first scattering, such as particle momenta and type, has traveled to the second one. This kind of information transport can continue over several scattering events.

This is a general problem of all transport codes, and is worsened because the gluon-gluon cross section becomes rather large for low energies (instead of vanishing). Along with the large gluonic cross sections are relatively large gluon densities which result in very high probabilities for scattering in subsequent time steps. Therefore information transport could be supported over relatively large distances without damping.

In many existing cascade codes first steps for dealing with the problem of superluminous signals have been taken: Most of the codes, including ours, allow only one interaction per particle per time step. This restriction is consequent and clearly justified since a time step is the shortest scale in the model. This restriction prevents signals from avalanching over huge volumes within only one time step.

A second restriction implemented in many codes is the

"closest approach" criterion. For a scattering process it demands in addition to "spatial distance within total cross section" also "the two particles have reached their point of closest approach assuming their current trajectories." Usually one would look at $|x^\mu x_\mu|$ with x_μ being the four-vector distance between the two particles involved, and demand that this quantity is minimal. As the two particles' positions are taken in the same time step this quantity reduces to the spatial distance squared. Even though this looks like a Lorentz-invariant criterion, it is not, since the conceptual necessity of taking both particles' position at the beginning of a time step (i.e., with vanishing time separation in the lab frame) is a non-Lorentz invariant restriction; see Sec. IV. Nevertheless, the "closest approach" restriction prevents causality violating signal transport in the longitudinal (parallel to the beam) direction, but unfortunately has no effect on the transverse direction.

To demonstrate those causality violating shock waves, the parton cascade simulation of a 100 GeV/nucleon (p,Au) collision was run with different constant cross sections and S-wave scattering. Figure 2 shows the distance of scattering events from the beam axis versus the simulation time for different cross sections. While during the initial stages of the collisions the outmost scattering events occur at distances larger than those allowed by causality arguments, the information transport soon appears to be damped. It turns out that this phenomenon is not — as one would expect — mainly due to a dropping of the collision rate, but rather to a form of random walk: only a fraction of the individual signal propagations lead outwards, others have the opposite effect, which results in an effective damping. In fact it turns out that the expectation value of the distance of scattering events from the beam axis is roughly proportional to the square root of the simulation time, which is a characteristic feature of random-walk mechanisms; compare the top panels of Fig. 2. This mechanism is a valid description until the cross sections are so large that the parton distribution basically appears
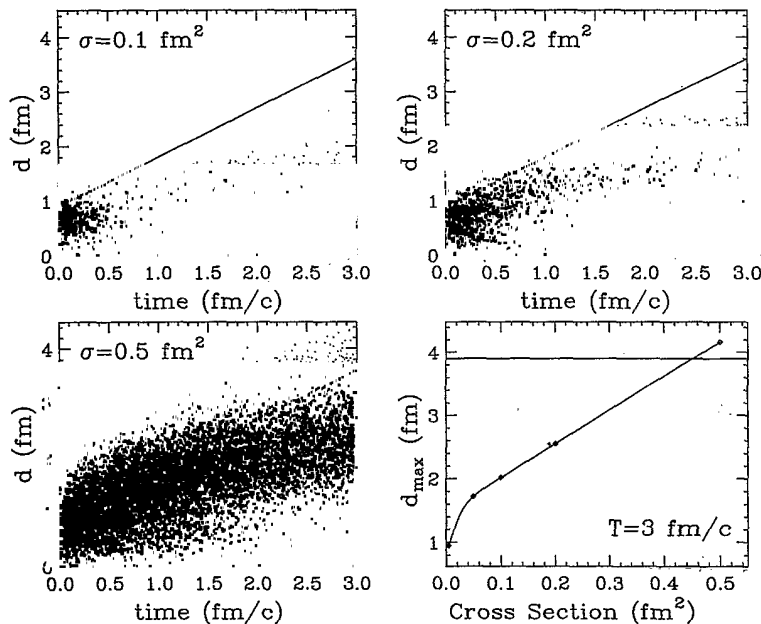

FIG. 2. Distance d of scattering events versus simulation time at constant cross sections of $\sigma = 0.1$, 0.2, and 0.5 fm^2. The solid line indicates the distance that could be reached by a signal that travels with the speed of light. One can clearly see the outwards traveling shock wave and how it gets damped out with time. For the smaller cross sections the causality violation is rather small and only present in the initial stages of the interaction. One should note that for realistic energy-dependent cross sections the initial scattering events take place with a lower cross section than the later ones because the c.m. energy is much higher. In the lower right panel the maximum distance $d_{\max}$ of scattering events from the beam axis is plotted versus the cross section σ. The horizontal line indicates a distance that during the simulation time could only be reached with the speed of light.

solid, in that limit the information travels outwards proportional to the simulation time; see the panel for $\sigma = 0.5$ fm^2. By the nature of random walks, the information expands fastest in the initial phase of the collision. With realistic energy-dependent cross sections, however, those initial scattering events happen at lower cross sections than the ones in the later stages due to the higher c.m. energy, which partly suppresses this initial outburst. Overall for $\sigma = 0.2$ fm^2 the causality violations are still rather moderate, for 0.5 fm^2 the effect becomes dominant.

Figure 2 also shows the maximum distance of scattering events from the beam axis as they occurred for different cross sections. As it turns out, this value depends linearly on the cross section for an extended range, beyond $\sigma \approx 0.4$ fm^2 the outmost scattering events occur at a distance that can only be reached with superluminous signal velocities.

III. MICROSCOPIC CAUSALITY VIOLATIONS

In addition to macroscopic causality violations such as superluminous shock waves, both the nonretarded interactions and the model inherent propagation of the whole particle configuration from one time step to the next lead to causality violations on the level of elementary scattering processes.

A Lorentz-invariant simulation of parton scattering would require a truly four-dimensional configuration space, in which an interaction can be established between any spacetime point of one parton's trajectory and any other spacetime point on another parton's trajectory. In the framework of classical fields, the scattering of two particles would be represented by their continuous change of trajectory in the retarded field of the respective other particle.

The actual realization of scattering events in the simulation only agrees in a certain limit with this model, namely if the two partons are coming from infinity with infinite rapidity and opposite directions: with increasing rapidity, in the lab frame the fields are distorted to pancakes with an orientation perpendicular to the trajectory, reducing the dominant part of the interaction between the particles to a shorter and shorter region along their trajectories. In the limit of infinite rapidity, the interaction between two partons traveling with a nonvanishing impact parameter in opposite directions would be reduced to a momentary interaction at the point of their closest approach, making them change their trajectories at equal times. This interaction would take place at a spacelike distance equal to the impact parameter — why does this not violate causality? The reason is, that the parton's field pancake — even though it is traveling along with its present position — is built up from contributions out of the parton's past, the respective other parton does not scatter from the field generated at the first parton's present position, but from a field component that was generated along the first parton's trajectory at a lightlike distance.

This limit agrees both with the claim of Refs. [2,3] that the interaction distance should be spacelike, because otherwise an interaction would influence the absolute past of one of the partons, and with the actual realization of scattering processes in the simulation: in the framework of a 3+1 dimensional transport simulation the distance of the testparticles is by the model itself determined to be spacelike. This

is because the information available at the beginning of a time step is no more than the points of the trajectories on a certain x, y, z hyperplane, as well as the corresponding momentum four-vectors of the particles, also only at that time coordinate. The lightcone of any one particle extends both before and after that hyperplane, but has no extension into that hyperplane itself, causing all other particles present in the simulation to have a spacelike distance from it.

But this limit soon loses its applicability: Staying in the model of interactions between the partons due to classical fields, as already pointed out, the field traveling with the partons is in fact built up from contributions out of their history, which for partons coming from infinity. results in Lorentz-contracted field pancakes. But in a cascade simulation it is highly unlikely that seen from a parton A, parton B already was on the same trajectory a lightlike distance ago. In fact, as the partons are nearly traveling with the speed of light themselves, spacetime points with lightlike distances along their trajectories can happen to be very long ago, which in connection with the high interaction rates makes the idealized picture of the field pancakes inapplicable. Changes in trajectories can make more than one point along the trajectory of parton B have a lightlike distance to parton A, the acceleration connected to the changes in trajectory of parton B generates additional fields. Even worse, through the mechanism of parton generation and absorption, parton B might not even have existed at lightlike distances from parton A, still within the framework of the transport simulation, scattering would be possible — and causality violating.

Also, as in the idealized picture the c.m. frame is moving parallel to the partons' trajectories and perpendicular to their distance at the point of closest approach, the equal-time character is true in both the lab and the c.m. frame. As soon as the two partons are not traveling into opposite directions, their spacial distance also leads to a time separation, making the scattering time different in the lab and c.m. frame.

IV. FRAME-DEPENDENCIES AND TIME-ORDERING

An obvious consequence of the model's causality violations is its frame-of-reference dependence: The simulation will for example certainly lead to different results when run in the rest frame of the target. This was already shown for the example of a $^{12}C + ^{12}C$ internuclear cascade calculation in Ref. [10], the authors demonstrated that both the total number of collisions and the individual time ordering of given collisions were frame dependent. As obvious that seems from the simple problems pointed out in Secs. II and III, for a parton cascade it is not yet the whole story: The simulation cannot even be run in the rest frame of any one nucleus, because there is no possibility to create appropriate initial conditions. The parton distribution in nucleonic matter is frame dependent, the higher the energy of a nucleon the higher the number of virtual partons. To put it in other words, usually components of the nucleonic wave function are considered a parton if they carry a momentum fraction beyond a threshold given by a minimum x value, the latter one being a parameter of the model. However, by boosting the nucleonic wave function into an accelerated frame of reference, a procedure described by the model parameter Q^2 of the parton distribution function $f(x, Q^2)$, more and more components
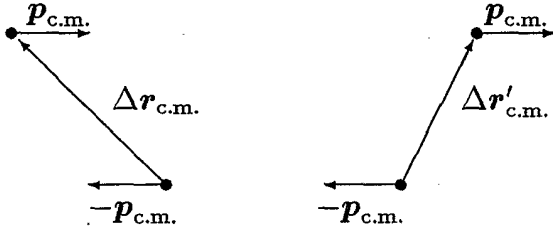
FIG. 3. Two partons passing their point of closest approach in the c.m. frame.

of it cross that threshold x value, leading to higher and higher parton numbers.

Therefore, when asking questions about how the collision of two partons looks in their rest frame as compared to the lab frame, another valid question is do those two partons even exist in the other frame? Or are in that frame other partons around that the collision partners would be much more likely to scatter with instead?

However, as this question cannot be addressed within the framework of a transport simulation, it is worthwhile to study the effects of a transformation of two given partons into their c.m. frame. It turns out that in addition to the above inconsistencies, by boosting the partons with β into their c.m. system, there they have a time separation of

$$\Delta t_{c.m.} = -\gamma \beta \cdot \Delta r_{lab}. \tag{4.1}$$

The partons' positions, being taken at equal time in the lab frame, will, unless β and Δr_{lab} are perpendicular, not be at equal time in their c.m. frame and vice versa. The construction of a "Lorentz-invariant CMS distance" as in Refs. [2,3] seems doubtful. This time separation can very well be larger than the transformed time step length, leading to a situation where the partons' positions are not taken within the same time step within the c.m. frame anymore. As a result, the closest approach criterion can only provide a means to get an averaged point in time for an actual scattering event.

For this criterion, described in Sec. II, one can choose to define it either in the particles' c.m. frame or in the lab frame (a third approach will be described in subsection VIF). Because of the nonvanishing time separation of the partons in their c.m. frame, the two possibilities are not equivalent. We compare both methods and find nevertheless no significant change in the collision rate, even though the individual collisions happening in both simulations are different. For our further simulations we have chosen the c.m. frame, since intuitively this frame seems to be more significant for the individual scattering events. In this frame, the scalar products of the momentum and the distance vector both at the beginning and at the end of the time step are to be calculated. If this scalar product changes sign, the position of closest approach is reached within this time step. In Fig. 3 $\Delta r_{c.m.}$ denotes the distance vector at the beginning of the time step, $\Delta r'_{c.m.}$ at the end. The criterion is $(p_{c.m.} \cdot \Delta r_{c.m.})(p_{c.m.} \cdot \Delta r'_{c.m.}) \leq 0$.

The nonvanishing c.m. time separation unfortunately also makes the calculation of $\Delta r'_{c.m.}$ ambiguous. In our model, the c.m. positions at the end of the time step are calculated by
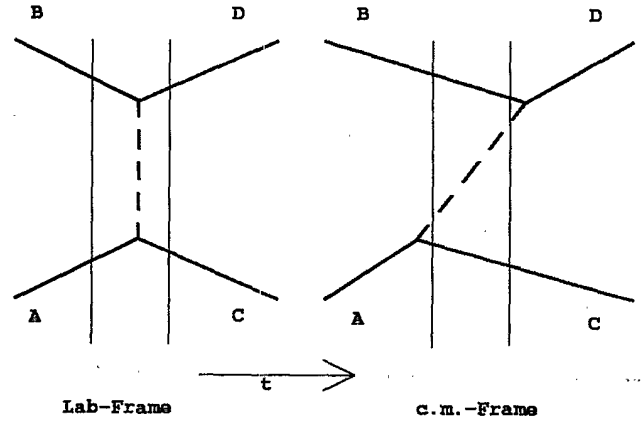

FIG. 4. Since a spacelike distance usually prevents causal dependencies of two spacetime points, in the c.m. frame the scattering of parton A can happen so much earlier than the scattering of parton B that at the beginning of the c.m.-frame's time step (denoted by thin vertical lines in the figure) parton A has already scattered while parton B has not yet scattered at the end of that time step. In the lab frame, however, at the beginning of its time step parton A and B have not yet scattered while at the end both have.

propagating the partons within the lab frame and boosting the result into the c.m. frame. The result, expressed in c.m. quantities, is

$$\Delta r'_{c.m.} = \Delta r_{c.m.} + \left(\frac{p_{c.m.}}{\gamma(E_{c.m.,1} + \beta \cdot p_{c.m.})} \right. $$
$$\left. + \frac{p_{c.m.}}{\gamma(E_{c.m.,2} - \beta \cdot p_{c.m.})} \right) \Delta t_{step}. \tag{4.2}$$

Due to the spacelike distance of the partons, however, the definition of "beginning" and "end of a time step" becomes frame dependent.

Consider a process where the partons A and B scatter and produce a parton pair C and D; see Fig. 4. In the lab frame this happens within one time step, at the beginning of the lab-frame's time step partons A and B are present, at the end partons C and D. In the transformed time step within the c.m. frame, however, this setup can easily be distorted to a situation where in the beginning of that time step partons B and C are present, and at the end partons C and D. Seen from yet another frame, in the beginning A and D could exist. One consequence is that in our simulation rescattering processes have to be explicitly forbidden: In spite of the closest-approach criterion rescattering would still be possible if two partons are scattered towards each other — as the distance between partons involved in a scattering event can very well be greater than $\Delta t_{step} c$, it is possible for those two scattered partons to again reach a point of closest approach in a later time step. In the case of a retarded interaction, this would not be possible.

More relevant than the time scale given by the time step, which is a model-dependent parameter, is the time scale given for example by the time it takes for the two nuclei to cross through each other, which is about 0.2 fm/c. This time interval corresponds to a parton-parton impact parameter of 0.2 fm beyond which the time ordering of scattering events is

frame-dependent. As the interactions in question happen between particles traveling into the same direction, those would also be low-energy interactions with cross sections very well in the range of such impact parameters. The effects of this frame-dependent time ordering of the incoming and outgoing particles of a scattering event have to be subject of extensive examination.

An interesting approach is that of Refs. [12,13]: In this method, configuration space is divided into boxes. Within the boxes the scattering partners are randomly chosen according to a probability that is a function of the cross section — convergence of this method towards the solution of the Boltzmann equation for an infinitely small box size and time step length, as well as an infinite number of test particles, is shown in Ref. [14]. The code of Ref. [13] was successfully made more efficient by only considering a fraction of the possible pair combinations within each box, and compensating the otherwise resulting loss in collision rate by an enhanced probability for the collision of the chosen pairs. The authors of Ref. [12] claim that this stochastic method of formulating the collision term is covariant since it is dealing with transition rates instead of geometrical interpretations, therefore no problems connected with the time ordering of processes would occur. In fact, since in the model the time order of processes is chosen randomly anyway, the model has no "right" time order that could be distorted by relativistic effects. However, this new approach does not overcome the problem of superluminous shock waves. Within a given cell of longitudinal size $\delta r_\parallel$ and perpendicular size $\delta r_\perp$ any two particles have a chance of colliding. Since the subsequent advection step may carry some of these into neighboring cells, the maximum transverse velocity for information transport will be $\delta r_\perp / \Delta t_{step}$. Since in general $\delta r_\perp^2$ is several times larger than the cross section σ, the resulting maximum possible causality violations in transverse direction are even larger than in the method discussed above. In addition, the stochastic method also allows for superluminous information propagation in longitudinal direction, with velocity $\delta r_\parallel / \Delta t_{step}$. Some of our recent studies indicate that in this approach actually the nuclear flow is very well dependent on the frame of reference the simulation is run in.

V. THE PARTON MODEL

Classical simulations, which have been successfully applied to heavy ion collisions at intermediate energies [15], are now [1–8] being extended to high energies. The main step in the extension of this microscopic model is using a parton based picture of the nuclei rather than a hadronic picture; consequently the interactions between the testparticles are to be described in the framework of QCD, leading to so-called parton cascades.

Our code works in 3+1 dimensions using fully relativistic kinematics for the partons, where the quarks are consequently treated as massive particles. Both quarks and gluons can be off shell. The initial conditions are determined by standard parton distribution functions $f(x,Q^2)$[16], where the value for Q^2 and the minimum x are parameters of the model. Technically stability of the incoming nuclei is guaranteed both by a coherent motion of all partons in longitudinal direction, and by the restriction that particles from the

same nucleus cannot scatter with each other before at least one of them has scattered with a particle from the other nucleus.

In this preliminary version of the code only QCD processes with two partons in the incoming and two partons in the outgoing state are implemented [9,17,18]. Phenomenological screening or cutoff masses have been added into the propagators to avoid divergent total cross sections. However, the gluon-gluon scattering cross section includes a four point diagram which does not contain a propagator. This means that the divergence in this cross section must be handled differently from the other cross sections. One usually regularizes the gluon-gluon cross section by setting it to a constant value below a certain cut-off energy, in our case we have chosen a cutoff of $s \approx 0.25$ GeV^2 corresponding to $\sigma \leq 0.45$ fm^2. This cutoff seems appropriate because it agrees both with a reasonable c.m. energy below which perturbative QCD loses validity, and with the limiting cross section for superluminous shock waves found in Sec. II. Other methods of cutting off these cross sections while maintaining the correct physics are being investigated. Also, no medium modifications to the elementary cross sections are taken into account. Figure 5 shows the cross sections being used. Our analytic expressions for cross sections have been checked in the massless quark limit against results from the literature [19,20], some of them also in the massive case [21].

VI. COMPARISON OF METHODS FOR DEALING WITH SUPERLUMINOUS SIGNALS

This section contains a comparison of different methods for dealing with the problem of superluminous signal transport and is the outcome of simulating central collisions of a 100 GeV proton on a 100 GeV per nucleon gold nucleus. This setup seems suitable since it allows observation of the information transport from the incoming (comparably small) particle in nuclear matter. Table I summarizes the parameters used for the simulations. The time step length of 0.0002 fm/c was determined by running the simulation with different time step lengths and observing the total number of collisions. It turned out that the number of collisions did not change significantly below the value chosen anymore, even though the simulation does not necessarily get more precise with smaller time steps due to the causality violating effects. With the values chosen for Q^2 and the minimum x value approximately 9000 partons per testrun are generated. For the following calculations, the longitudinal extent of the nuclei in our model is determined by the Lorentz contraction only, Fig. 6 shows the initial configuration in the lab-frame and 1 fm/c later. The effects of "wee partons" are examined in the last subsection. The cross sections were energy dependent according to Sec. V and Fig. 5.

The simulation was first run for S-wave scattering in the expectation that this would be the worst case. Compared to the realistic forward peaked angular distributions, S-wave scattering favors transverse signal propagation. However, it turned out that the angular distribution hardly makes any difference as far as causality violating effects are concerned, the only noticeable change was in the final rapidity distributions, where it turned out that the gap in rapidity between unscattered and scattered partons was wider for S-wave scat-
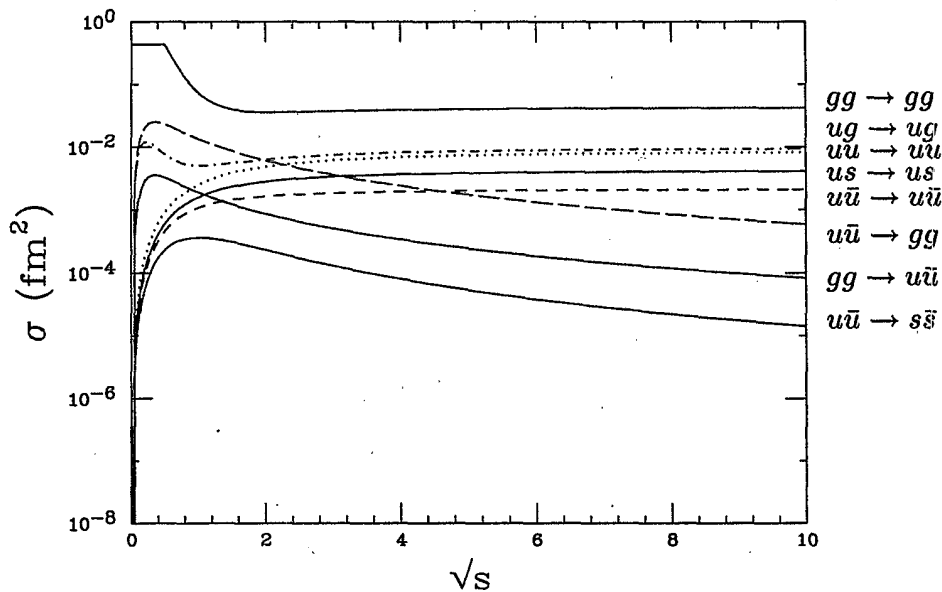
FIG. 5. Example of partial cross sections being used versus the c.m. energy $\sqrt{s}$. The gluon-gluon cross section is divergent for $\sqrt{s} \to 0$, a problem that cannot be solved with the introduction of cutoff masses. The cross section was chosen to be constant below $s = 0.25$ GeV^2 at a value of approximately 0.45 fm^2.

tering: the partons lose more units of rapidity in the initial collisions. The small effect of the angular distributions is understandable from the fact that even isotropic distributions in the c.m. frame are strongly forward peaked in the lab frame.

The top row of Fig. 7 summarizes the results for a simulation with a realistic angular distribution. The top left histogram shows the signal velocity distribution regarding directly subsequent collisions; see Fig. 1. In other words, with $r_{n,i}^\mu$ being the position of the ith collision of the nth particle, the distribution of

$$v_S(n,i) := |r_{n,i} - r_{n,i-1}| / (t_{n,i} - t_{n,i-1}) \qquad (6.1)$$

for all n and $i > 1$ is shown. The solid histogram shows the radial component of those velocities, the dashed histogram includes the longitudinal component—the strong peak at c results from processes for which the signal transport was dominated by the partons' motion with the respective nuclei. On the order of 50 isolated scattering events with velocities from $50c$ up to $1360c$ have been suppressed in the plot.

TABLE I. Parameters used for the comparisons.

| Parameter	Chosen value
Total time of simulation	3 fm/c
Time step length	0.0002 fm/c
Number of time steps	15000
Proton energy	100 GeV
Energy per nucleon Au	100 GeV
Impact parameter	0 fm
Minimum x value for $f(x,Q^2)$	0.005
Q for $f(x,Q^2)$	25 GeV
Bag radius for nucleons	0.9 fm
α_s	0.2
Cutoff mass for gluon propagators	1.0 GeV
Cutoff mass for quark propagators	0.2 GeV
Number of parallel test runs	5
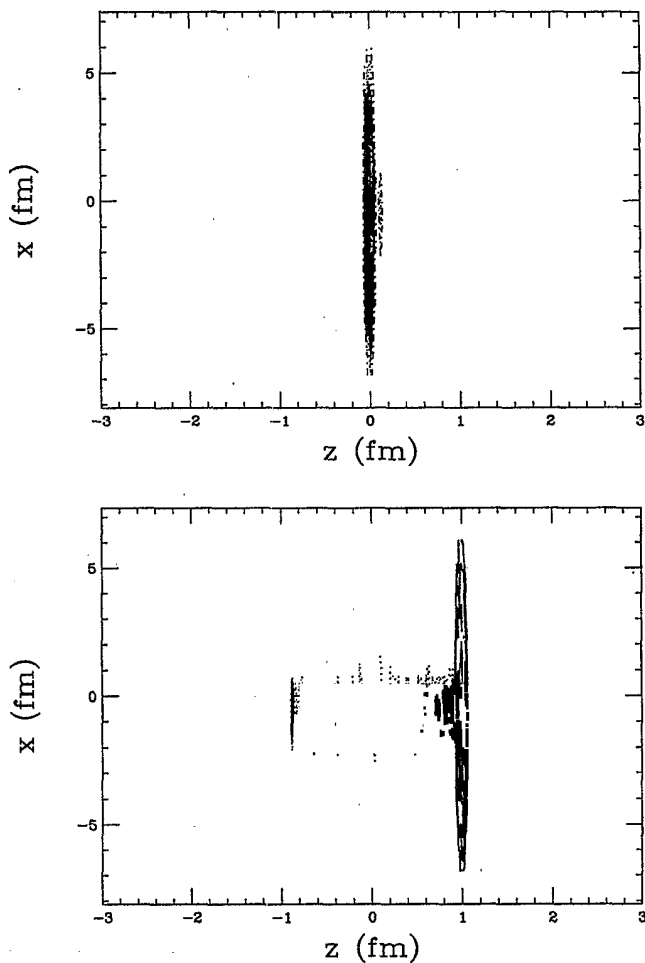
FIG. 6. In the top panel the projection of the initial parton configuration on the (x,z) plane is depicted. The highly Lorentz-contracted proton is moving to the left into the equally contracted gold nucleus which is moving to the right. The bottom panel shows the configuration 1 fm/c later.
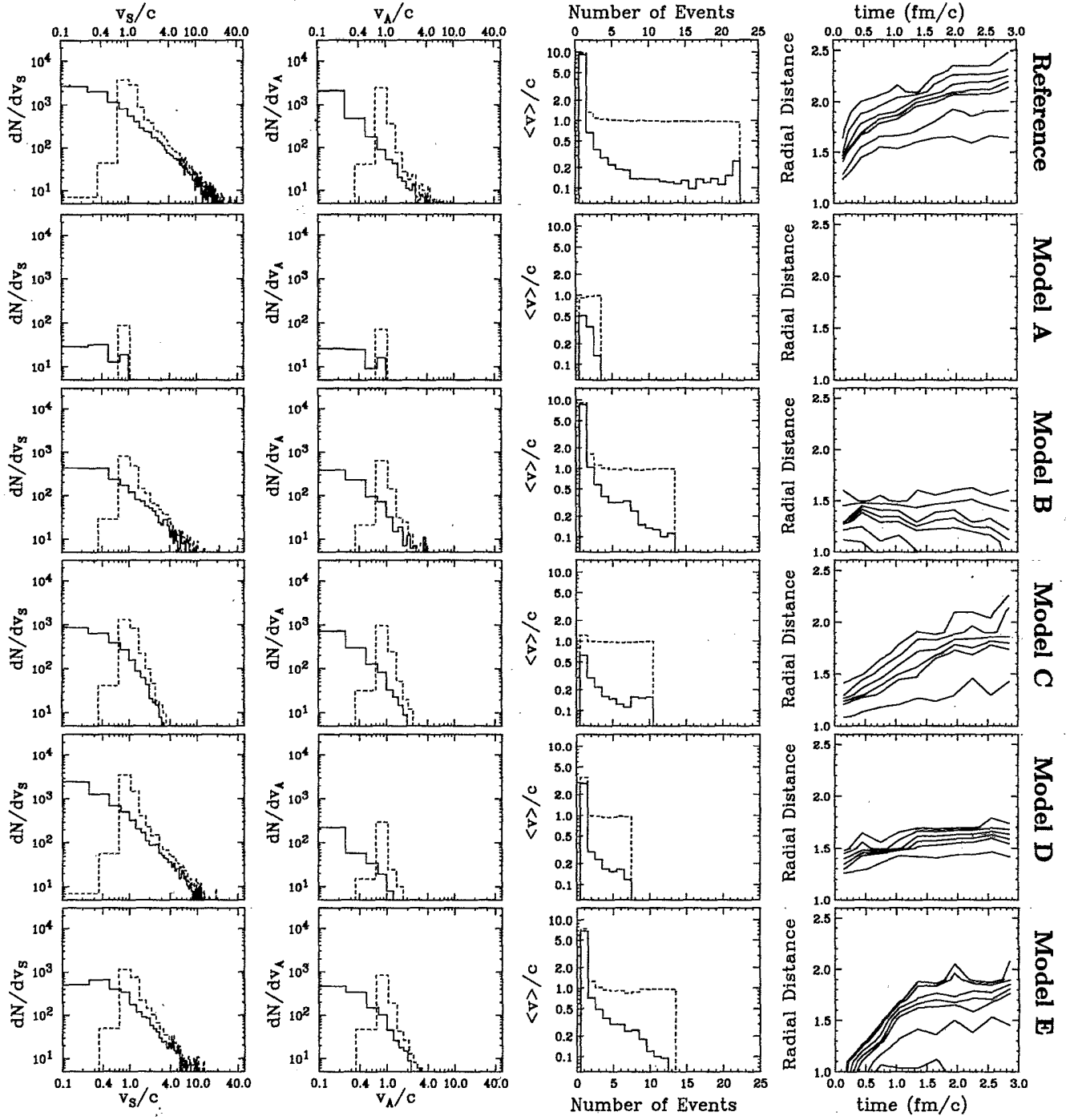
FIG. 7. Results of simulations with different mechanisms to suppress superluminous signal transport. The leftmost histogram shows the signal velocity distribution regarding directly subsequent collisions, v_S; see Fig. 1. The solid histogram shows the radial component of those velocities, the dashed histogram includes the longitudinal component. The second panel shows a more general impression of the signal velocities, in this histogram the signal velocity v_A from the very first to the very last scattering event that a parton was involved in is calculated. Again, the solid histogram shows the radial component of the signal velocities, the dashed histogram also takes into account the longitudinal components. The third panel shows how subsequent scattering events are leading to this overall damping of peak velocities occurring in single scattering events: again starting from the very first scattering event of a parton, the average signal velocity $\langle v \rangle$ to the ith following scattering event of the partons is calculated; both the total and only the radial component of the velocities are shown. Finally, the rightmost panel shows the outgoing shock wave, in a plot of distance from the beam axis versus simulation time the contour lines of the scattering event distribution are given. For model A, the rejection of any individual scattering events that would lead to superluminous signal transport, the shock wave was so strongly damped that it did not even go beyond the radius of the incoming proton.

The second panel shows a more general impression of the signal velocities. Instead of just taking into account the signal velocity occurring within one single scattering event, in this histogram the signal velocity from the very first to the very last scattering event that a parton was involved in is calculated. With the notation from above and $N(n)$ being the number of collisions that the parton n was involved in, the distribution of

$$v_A(n) := |r_{n,N(n)} - r_{n,1}| / (t_{n,N(n)} - t_{n,1}) \qquad (6.2)$$

for all n is shown. Again, the solid histogram shows the radial component of the signal velocities, the dashed histogram also takes into account the longitudinal components.

Because of damping effects the average velocities are much smaller than the velocities from one event to the next, the third panel shows how subsequent scattering events are leading to this overall damping of peak velocities occurring in single scattering events: again starting from the very first scattering event of a parton, the signal velocity to the ith following scattering event of the partons

$$v(n,i) = |r_{n,i} - r_{n,1}| / (t_{n,i} - t_{n,1}) \qquad (6.3)$$

is calculated, and the average $\langle v \rangle(i)$ over all particles n that had an ith collision is shown; again both the total and only the radial component of the velocities are plotted.

Finally, the rightmost panel shows how information is traveling outwards. The outer boundary of its spreading is after a very fast expansion in the first few tenth of a fm/c traveling with approximately $0.17c$. The maximum distance of a scattering event from the beam axis is 2.5 fm. A more detailed analysis of the overlay of the average c.m. energy and the distance of scattering events from the beam axis shows that the expansion of a shock-wave begins rapidly immediately after the c.m. energies get smaller, but then is damped out — only the initial stages of the collision seem to be problematic. However, one should note that in the later stages the individual collisions happen with very high signal velocities, and that it is rather by the random-walk character of the signal propagation over longer distances that the information does not travel with the same high velocity; compare Sec. II.

A. Restrictions on the signal velocity

An obvious way to avoid superluminous signal velocities is to systematically suppress all scattering events that would lead to signal velocities faster than the speed of light; the second row of Fig. 7 summarizes the results of this simulation.

It is not surprising that the velocity restriction leads to a huge reduction in the collision rate: While in the first stages of the collision the collision rate drops to 49% of the original rate, it drops in the later stages to only about 8% of the original rate, there is no outwards traveling information at all — it would be unwise to apply such an unjustified prescription given the huge effect, even more so, as from the extrapolation of intermediate energy results one would expect a rather strong outgoing effect of the proton impact.
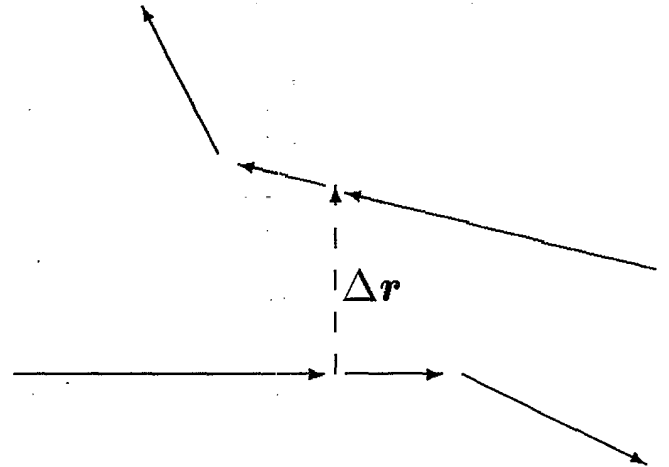

FIG. 8. A first step to the introduction of retarded interactions: After the scattering took place, the partons maintain their momentum for a time period of $|\Delta r|/(2c)$ in which they are not able to scatter with other partons. Only after this time the momenta are transferred to the partons.

B. Suppressing of low energy collisions

Once a parton has scattered with a parton from the other nucleus it can scatter with fellow partons from the same nucleus at much lower c.m. energies. Soft processes between partons from the same nucleus are problematic since the elastic gluon-gluon cross sections at low energies are large; systematically suppressing these reactions by placing a c.m.-energy cutoff on the scattering events should also suppress high signal velocities. For this model calculation the cross sections are set to zero below 0.4 GeV; see the third row of Fig. 7. The outcome of this simulation proves that indeed the shock-wave travels outwards through those low energy collisions, only the initial outburst remains.

In fact this model provides a way to address the problem of the energy-dependent parton resolution described in the beginning of Sec. IV: Disregarding interactions below a certain c.m.-energy cutoff could also be viewed as disregarding the interaction partners. By smearing out the step function of the cutoff to a smoother function that determines the probability of scattering events in dependence of the c.m. energy, one could try to simulate the behavior of the parton distribution function in dependence of the resolution parameter Q^2. However, other physics would have to take the place of the QCD interactions, in this lower-energy regime nucleonic interactions take over and hadronization patterns must be applied.

C. First steps towards a retarded interaction

As already pointed out, the main reason for the superluminous signal velocities is the instantenous character of the elementary interactions. To consequently overcome this problem no theoretical framework with time delays has been developed so far for parton systems, although some simple hadronic examples have been worked out. To estimate the effects of retardation it nevertheless seems appropriate to introduce a simple — but unphysical — way of time delay in the interactions: After an interaction took place the momen-
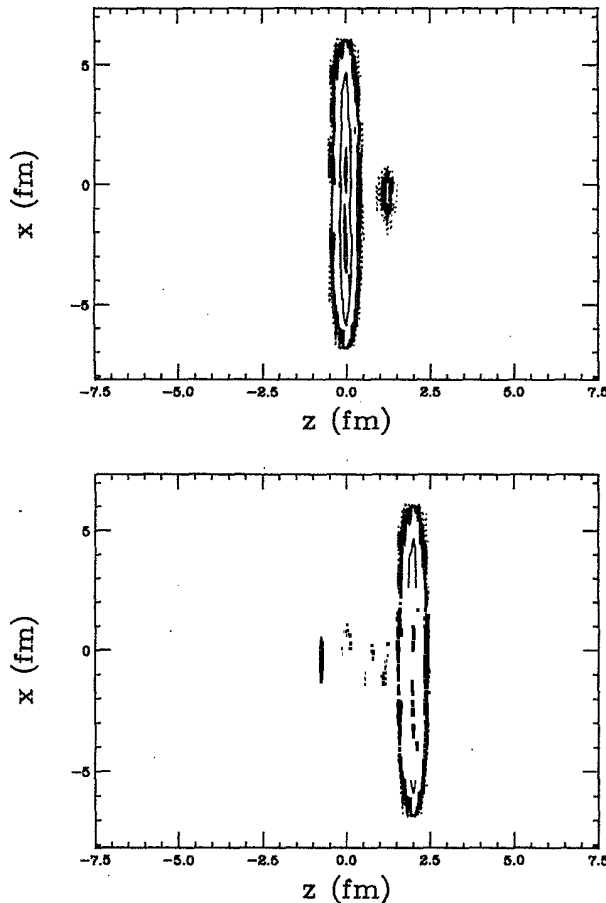
FIG. 9. Initial configuration and configuration after 2 fm/c for a simulation with wee partons.

tum transfer to both partons involved is delayed by $|\Delta r_{lab}|/(2c)$, where Δr_{lab} is the distance vector in the lab frame. In the meantime the partons are considered not being able to interact; see Fig. 8. A technical problem in our calculations, however, is that the time delay has to be implemented for integer numbers of time step lengths and therefore does not necessarily fully correspond to its supposed length.

It turns out that the propagation of the outgoing shock wave becomes more homogeneous, the initial outburst is suppressed while the distances of the outmost scattering events are comparable to the simulations with instantaneous interactions; see the fourth row of Fig. 7.

D. Downscaling the cross sections

The maximum signal velocity is proportional to the maximum cross section. Downscaling the cross sections to $1/n$th of its original value and compensating this by the initialization of n times as many test partons leads to a reduction of the maximum signal velocity by $1/\sqrt{n}$. Due to limitations given by the increasing computation time, for this model calculation we have chosen a factor of only $n=5$ which corresponds to a reduction of the maximum signal velocity by a factor of ≈ 0.45.

It turns out that this technique radically changes the characteristics of the simulation, the outgoing shock wave is strongly suppressed; see the fifth row of Fig. 7. This outcome is surprising, since Ref. [24] found that for internuclear cascade codes the outcome of this "full-ensemble" method (n times as many test particles) is comparable to the usual "parallel-ensemble" method (n parallel test runs). In the case of parton cascades apparently this does not hold true anymore due to the reduction of superluminous signals.

Before favoring a method however that leads to such strong changes in the outcome of the simulation, further analysis is mandatory.

E. Wee partons

When initializing the parton configuration the Lorentz-contraction leads to very thin pancakes of nuclear matter, the contracted thickness of a nucleon is around 8×10^{-3} fm, that of the gold nucleus 6×10^{-2} fm. Thereby the z coordinate of the partons is fixed rather precisely. However, the momentum of the low x components of the nucleonic wave function is also determined within the order of a few hundred MeV. This leads to a violation of the uncertainty principle, which lead to the suggestion that in any frame of reference the nucleonic wave function should be smeared out to a pancake thickness of at least approximately 1 fm, where the low x components are situated further outside and only the valence quarks are actually within the highly contracted pancake [4–8,22,23]. Applying this kind of initial configuration naturally leads to a smaller parton density; in our case approximately by a factor of 20. Figure 9 shows the parton configuration both at the beginning of our simulation and at 2 fm/c.

One's hope can be that the increased width and smaller parton density of the nuclei compared to the fully Lorentz-contracted model helps to eliminate some causality violating effects; see the bottom row of Fig. 7: The initial outburst of a shock wave at impact is eliminated because the nuclei enter each other rather gradually, an outgoing shock wave within the respective nuclei is stronger damped because of a decrease in collision rate, and finally time-ordering problems on the scale of the time the nuclei are passing each other are rarified because that time scale becomes much longer.

However, there are now other inconsistencies: Although this concept given by the uncertainty relation is truly valid in any frame of reference, within this model there is no way of implementing it in a Lorentz-invariant way. In reality the components of the wave functions transform; in different frames different components of the wave function are considered a parton. In our model only the parton coordinates and momenta transform, while the partons themselves, once generated, exist in any frame. While for the initial collisions the c.m. frame of individual parton collisions nearly coincides with the lab frame, in subsequent collisions the c.m. frames are closer to the rest frames of the respective nuclei—in its rest frame, however, a nucleon, smeared out to 1 fm in the lab frame, has a longitudinal radius of 100 fm.

F. Proper time approach

As already pointed out, a fully covariant description of a particle collision would require a fully four-dimensional configuration space. This is not possible without giving up the

equal-time character of the simulation. Reference [10], however, proposes a causality preserving scheme that while retaining the unique global time character of the simulation minimizes the frame dependence of the choice of collisions partners for the particles, but not the frame-dependent time ordering of those collisions. Each particle i is considered to have its own clock showing its proper time τ_i,

$$d\tau_i = dt\sqrt{1-\beta_i^2(t)}, \quad \tau_i(t) = \int_0^t dt'\sqrt{1-\beta_i^2(t')}. \tag{6.4}$$

Since the particles do not change their momenta between collisions, the above integral can be reduced to a sum of products of the type $\beta_{i\alpha}\Delta t_\alpha$. With $\tau_{ic}(j)$ being the proper i time of the collision of particle i with particle j, and τ_{i0} being the proper i time of the most recent collision of particle i, let

$$\delta\tau_i(j) := \tau_{ic}(j) - \tau_{i0} \tag{6.5}$$

be the proper time distance between those two events, a Lorentz-invariant quantity. The collision instant $\tau_{ic}(j)$ is defined individually within the rest frame of particle i through the closest approach to particle j—in the other methods, the closest approach is defined either within one frame, usually the lab frame or the c.m. frame of the nuclei, or within the respective c.m. frame of a particle *pair*. In our previous discussions, we had chosen the latter mechanism. To corelate the individual closest approach tests, for collisions only the particle pairs (i,j) are considered for which both

$$\delta\tau_i(j) = \min\{\delta\tau_i(l) > 0, \quad l = 1, \ldots, N; l \neq i\} \tag{6.6a}$$

and

$$\delta\tau_j(i) = \min\{\delta\tau_j(l) > 0, \quad l = 1, \ldots, N; l \neq j\}, \tag{6.6b}$$

N being the total number of particles in the simulation. Through the restriction $\delta\tau > 0$ only collisions in the absolute future of each particle are considered. What the two above conditions mean is that for particle i the very next possible collision (in the sense of the proper time) is with particle j *and vice versa*. This algorithm only allows collisions that have no risk of not happening in another frame. Suppose particle 1 has a minimum proper time distance to particle 2, but particle 2 has its minimum proper time distance to particle 3, then no collision will take place at all.

The search for the very next collision partner of every particle in the simulation is an unavoidable N^2 problem. Since each of these tests involves a change of coordinate

system, this mechanism is computationally very intense. Therefore, it was only possible to simulate the initial stages of one single (p, Au) collision. We observed that the number of collisions in this phase dropped dramatically, in our test run to about 10% of the number in the other simulations; due to computational limitations, however, we are not able to claim significant statistics on this percentage. This outcome is compatible with the conjecture of the authors of Ref. [10] that the mechanism might underestimate the number of collisions [11]. In smaller simulations of (p,p) collisions we indeed observed situations where particle 1 had particle 2 as its closest collision partner, particle 2 had particle 3, and particle 3 again had particle 1. "Ring" configurations like this, possibly spanning over even more particles, might lead to the underestimation of the collision rate. This effect might have been enhanced by the high particle density and the extreme Lorentz contraction of the nucleons as compared to lower energy internuclear cascades the mechanism was developed for. Further investigation of this method is required, but due to computational limitations was not possible within this work. It is, however, not expected that the above mechanism can overcome the macroscopic problem of shock waves.

VII. CONCLUSIONS

The influence of superluminous signal velocities on the signal propagation in parton cascade codes was found to be smaller than expected. This is mainly due to two effects: In the initial stages of the interaction the energy-dependent cross sections tend to be small. Without this beneficial effect the signal propagation has a threshold in the region between 0.4 and 0.5 fm^2 from where on the velocity of the outgoing shock wave reaches the speed of light. In the later stages of the interaction shock waves get damped out not because of a lack of interactions but because of signal propagation that resembles a random walk: not every collision actually leads to an outward propagation, in fact, the equally probable inward propagation leads to a virtual damping of the shock wave.

In the near future the influence of particle production and particle absorption will be examined.

[1] U. Kalmbach, T. Vetter, T. S. Biró, and U. Mosel, Nucl. Phys. A563, 584 (1993).

[2] H. Sorge, H. Stöcker, and W. Greiner, Nucl. Phys. A498, 567c (1989).

[3] H. Sorge, H. Stöcker, and W. Greiner, Ann. Phys. 192, 266 (1989).

[4] K. Geiger and B. Müller, Nucl. Phys. A544, 467c (1992).

[5] K. Geiger, Proceedings of the XXVI International Conference

on High Energy Physics, Dallas, Vol. 1, p. 977.

[6] K. Geiger, Phys. Rev. C **49**, 3234 (1994).

[7] K. Geiger and B. Müller, Nucl. Phys. **B369**, 600 (1992).

[8] K. Geiger, Phys. Rev. Lett. **71**, 3075 (1993).

[9] J. Murray, G. Kortemeyer, S. Pratt, K. Haglin, and W. Bauer, NSCL/Cyclotron Laboratory Annual report 1994, p. 51.

[10] T. Kodama, S. B. Duarte, K. C. Chung, R. Donangelo, and R. A. M. S. Nazareth, Phys. Rev. C **29**, 2146 (1984)

[11] T. Kodama (private communication).

[12] A. Lang, H. Badovsky, W. Cassing, U. Mosel, Hans-Georg Reusch, and Klaus Weber, J. Comp. Phys. **106**, 391 (1993).

[13] P. Danielewicz and G. F. Bertsch, Nucl. Phys. **A533**, 712 (1991).

[14] H. Badovsky, Eur. J. Mech., B/Fluids **8**, 41 (1989)

[15] G. F. Bertsch and S. Das Gupta, Phys. Rep. **160**, 189 (1988).

[16] Version 2 CTEQ distribution function in a parametrized form, J. Botts, H. L. Lai, J. G. Morfin, J. F. Owens, J. Qiu, W.-K.

Tung, and H. Weerts, CTEQ Collaboration.

[17] J. Murray, G. Kortemeyer, S. Pratt, K. Haglin, and W. Bauer, NSCL/Cyclotron Laboratory Annual report, 1993, p. 61.

[18] G. Kortemeyer, J. Murray, S. Pratt, K. Haglin, and W. Bauer, NSCL/Cyclotron Laboratory Annual report, 1993, pp. 63,65.

[19] R. D. Field, *Frontiers in Physics: Applications of Perturbative QCD* (Addison-Wesley, New York, 1989).

[20] B. L. Combridge, J. Kripfganz, and J. Ranft, Phys. Lett. **70B**, 234 (1977).

[21] E. Eichten, I. Hinchliffe, K. Lane, and C. Quigg, Rev. Mod. Phys. **56**, 579 (1984).

[22] K. Geiger (private communication).

[23] L. McLerran, *Quark Matter and Heavy Ion Collisions; Bielefeld Workshop 1982* (World Scientific, Singapore, 1982), p. 63.

[24] G. Welke, R. Malflied, C. Gregoire, M. Prakash, and E. Suraud, Phys. Rev. C **40**, 2611 (1989).